DESIGN AND DEVELOPMENT OF POROUS TiMoZr ALLOY

By

Rabail Badar Abbasi

Bilawal Mushtaq

Muhammad Talha Faiz

School of Chemical and Materials Engineering

National University of Sciences and Technology

2020

1. Binding side spine:

   on top **FYP Report** Center **UG-ME-09** Bottom **2020**

DESIGN AND DEVELOPMENT OF POROUS TiMoZr ALLOY

By

(Leader – 193306 Rabail Badar Abbasi)

(Member 1 – 175508 Bilawal Mushtaq)

(Member 2 – 186636 Muhammad Talha Faiz)

School of Chemical and Materials Engineering (SCME)

National University of Sciences and Technology (NUST)

H-12 Islamabad, Pakistan

July, 2020

CERTIFICATE

This is to certify that work in this thesis has been completed by Ms. Rabail Badar Abbasi, Mr. Bilawal Mushtaq and Mr. Muhammad Talha Faiz, under the supervision of Dr. Khurram Yaqoob and Dr. Usman Liaqat at the school of Chemical and Materials Engineering (SCME), National University of Science and Technology, H-12, Islamabad, Pakistan.

Advisor:

Dr. Khurram Yaqoob
Department of Materials Engineering
School of Chemical and Materials Engineering
National University of Sciences and Technology

Co-Advisor

Dr. Usman Liaqat
Department of Materials Engineering
School of Chemical and Materials Engineering
National University of Sciences and Technology

Submitted Through:

HOD-------------------------------------

Department of Materials Engineering
School of Chemical and Materials Engineering
National University of Sciences and Technology

Principal/Dean -----------------------
School of Chemical and Materials Engineering
National University of Sciences and

Dedication

We would like to thank our respective families and teachers for guiding us throughout the process of this project and being a constant source of support.

Acknowledgements

All praise to Almighty-Lord, for His help and utmost support for the completion of this work.

We wish to pay our gratitude to our supervisor **Dr. Khurram Yaqoob,** whose support, and guidance allowed us to work to the best of our abilities. Under his supervision, we were able to expand and polish our set of skills.

We would also like to extend our thanks to **Dr. Usman Liaqat,** whose constant efforts and support contributed to the completion of this project.

Our sincerest thanks to **Muhammad Zafar Khan,** for providing valuable input, throughout the progress of this project.

Abstract

Titanium and its alloys have been widely used in the biomedical industry due to their attractive set of mechanical properties and biocompatibility. Beta-Ti alloys are more desirable due to their inherent lower young's modulus which reduces or eliminates the phenomenon of stress-shielding, whereby natural bone loses its strength by resorption, due to implantation of stiffer material beside it. Therefore, it is necessary for such a material to be synthesized which exhibits stiffness equal or close to that of the natural bone. One way of reducing the young's modulus of an alloy is to introduce porosity. In this project, we are focused on the modification of the ternary alloy system of Titanium-Molybdenum-Zirconium to produce a bio-implant that has optimum mechanical properties. The young's modulus is lowered by introducing porosity into the alloy by selective dealloying. A specific filler is added to the alloy composition in an increasing quantity, from TMZ5 to TMZ25 (increments of 5), to find the optimum percentage of filler required. Characterization of the alloy prior to and after dealloying is done by X-ray Diffraction Technique, Scanning Electron Microscopy, and results are compared. XRD and SEM results show that efficient distribution of filler material is achieved with subsequent efficient distribution of porosity within the alloy.

Table of Contents

List of Figures

List of Tables

CHAPTER 1

INTRODUCTION

1.0 Historical development of Bio-medical Alloy

From early ages, body implants are being utilized to replace natural body parts. The use of implant trace back to Egyptian and South American Civilization. At early times, dental implants of stone and ivory teeth were being utilized. But these implants provided great danger to human body as there was no safety measures and cleanliness related to the procedure. These implants had adverse effects on the human body instead of resolving the issue at hand. So, there was still plenty of room available for advancement.

As humans gained more knowledge, notable advancements were made in the field of bio-implants. With more technological innovation and research, different classes of implants have been introduced which include polymers, ceramics, metals and composite materials. Each type of material possesses unique properties which can be utilized according to the need of implant properties and location inside the body. The demand of metallic implant these days is more than ever due to the continuous growth of world population, traffic accidents and desire of people to sustain same level of lifestyle and activity. The total number of hip revision surgeries between 2005 and 2030 is expected to increase to 137% and that o knee revision surgeries by 607%.

1.1 Metallic Implants

The use of metallic materials for medical implants dates back to the 19^{th} century, leading up to the era when industrial revolution began. The demand of metallic implants for bone replacement and fixation led to the advancement in field of metallic implants. The most notable class of bio-implant is metals as they possess superior properties. Despite having numerous metals and alloy systems, only a few are bio-compatible and FDA approved metals which can only be utilized for implant.

Most notably these classes of metals include Titanium based alloys, Cobalt based alloys and Stainless-steel alloys and miscellaneous. All of these categories of metallic implants possess unique properties with having minimum adverse effect on body. These implants are routinely being applied to human bodies. [6]

Figure 1 - Metallic hip implant

1.1.0 Stainless steel

Stainless steels were widely being used as orthopedic implant due to ease of fabrication and corrosion resistance. The FDA approved stainless steels are 316, 316L, 317 and317L. The most used class of stainless steel are 316L which contain Fe; 16-18.5%Cr; 10-14%Ni; 2-3%Mo; <2Mn; <1Si; <0.003C. However, 316L is not preferred for permanent load bearing applications as it shows poor wear resistance, low fatigue properties and has inferior corrosion resistance when in contact with body fluid for longer period of time, and creates toxic by-products. Due to presence of nickel and chromium, toxicity and carcinogenicity is an issue. So, it is being replaced by nitrogen variants of stainless steel, titanium-based alloys and cobalt-based alloys as they have superior corrosion resistance and fatigue properties.

The 316 L stainless steel, due to ease of fabrication and relatively low cost is still being used in non-permanent devices such as bone plates, internal fracture fixation and bone screws.[4]

1.1.1 Cobalt based alloys

Cobalt based alloys show superior mechanical properties namely fatigue resistance, temperature endurance, strength and wear resistance compared to stainless steel due to presence of HCP and FCC closely packed structures. Cobalt is alloyed with chromium which gives passive layer due to formation of chromium oxide, resulting in high corrosion resistance. Other alloying elements like nickel, iron, carbon and silicone are also preset in minute quantity. Molybdenum up to 5-7% is also intentionally added to obtain uniform grain size to achieve good mechanical properties.

The cobalt based alloys show good balance between biocompatibility and mechanical properties coupled with high cost of manufacturing. These alloy systems are used where high wear resistance and high load bearing applications are required with longer duration of contact with body fluids such as knee and hip joint replacement. [4]

1.1.2 Titanium-based alloys

Titanium and its alloys show higher level of biocompatibility as titanium is corrosion resistant due to presence of naturally occurring oxide layer. Its alloy systems show high mechanical strength and relatively low specific density (4.5 g/cm^3). The elastic modulus of titanium and its alloys is relatively lower than that of stainless steel and cobalt based alloys which help to avoid stress shielding when used as implants. Different alloying elements are added in titanium to act as alpha stabilizers or beta stabilizers. Elements like Al, Ga and Sn stabilizes the alpha phase which has HCP structure. The alpha phase shows good corrosion resistance but limited mechanical resistance. Whereas, V, Ta, Mo, W, Cr, Fe act as beta stabilizer having BCC crystal structure. Beta phase shows lower young’s modulus which helps in avoiding stress shielding. Commercially pure titanium and its alloys are being used in hip joint replacement, orthopedic and dental implants, etc. However, there is still room for more research and improvement in titanium-based alloys. [5]

1.1.3 Advantages and Disadvantages of metallic implants

Advantages	Disadvantages
• High Strength	• corrosion
• Fatigue resistance	• High density
• Wear resistance	• High modulus
• Ease of fabrication	• toxicity

Table 1 - Advantages vs Disadvantages of metallic implants

1.2 Issues related to metallic implants

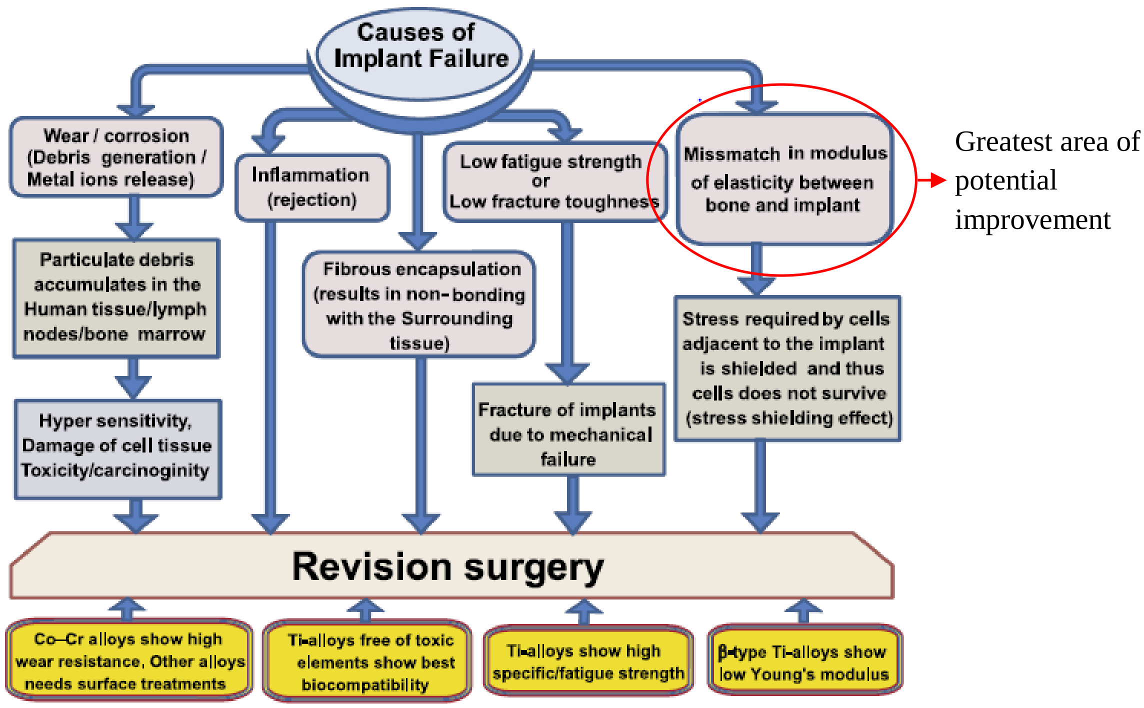

Figure 2 - Causes of Implant Failure

Among the polymers, ceramics, composites and metallic implants, metallic implants are preferred due to many positive factors associated with metals. These positive factors include ease of manufacturing, good fatigue and wear properties, abundance, etc. However, there are still number of issues related with metals due to their compositional and structural properties. These issues are still being investigated and improved through research. Few nominal issues related with metallic implants are as follows:

1.2.0 Osseo integration

Osseo integration refers to the interface between the metallic implant and the surrounding bone tissue. Good osseo-integration is required in order to achieve optimum functionality of implant. Osseo integration is a time taking process which is obtained by going through mechanism named as inflammation phase, proliferative phase and maturation phase. A stable bond between the bone tissue and implant depends on surface chemistry, surface roughness, surface area and surface topography of implant. The implant should provide suitable conditions for tissue to proliferate and form a stable bond. Otherwise, it will result in loosening of implant which can cause complications. [3]

Figure 3 - Tissue interaction with implant

1.2.1 Stress shielding

The modulus of elasticity of metals is relatively high as compared to that of bone. This difference gives rise to stress shielding: When the implant is integrated next to a bone, upon application of load, due to higher modulus of elasticity of implant, the implant absorbs most of the load. This in turn causes removal of stress transfer to the bone leading to reduction in bone density (osteopenia). This weakening of bone is not beneficial and causes problems. This can be avoided by bringing the modulus of elasticity of implant closer to

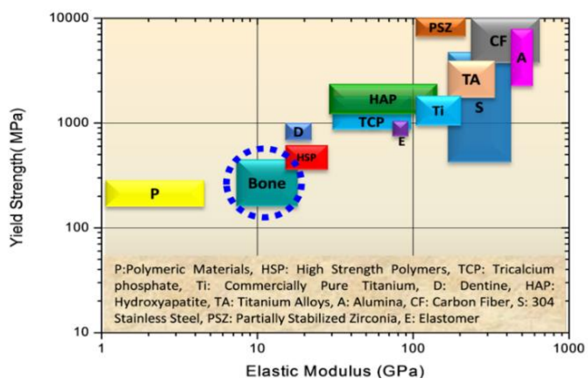

Figure 4 - Elastic Modulus of metals in comparison to cortical bone

that of bone. There are various techniques for reducing the modulus of elasticity such as reducing density by introducing porosity. There is still a lot of research being conducted for achieving low modulus through different routes.[8]

1.2.2 Corrosion

Corrosion of implant from contact of body fluids releases by-products, taken up by body fluids, inside the body. Depending upon the nature of byproducts, they can either cause no adverse effect in the body or can cause toxic effect such as inflammation, carcinogenicity, etc. The corrosion rate of the implant depends upon various factors including type and velocity of body fluid in contact with the implant. For instance, nickel present in stainless steel implants and cobalt based implants results in toxicity upon corrosion. The corrosion of the implants should be avoided by using right implant with good resistance to corrosion. Implants can be made corrosion resistance by addition of alloying elements. [11]

1.2.3 Aseptic loosening

Aseptic loosening is the failure of bond between implant and surrounding tissue over the course of time [14]. It can occur due to inadequate initial fixation, mechanical loss of

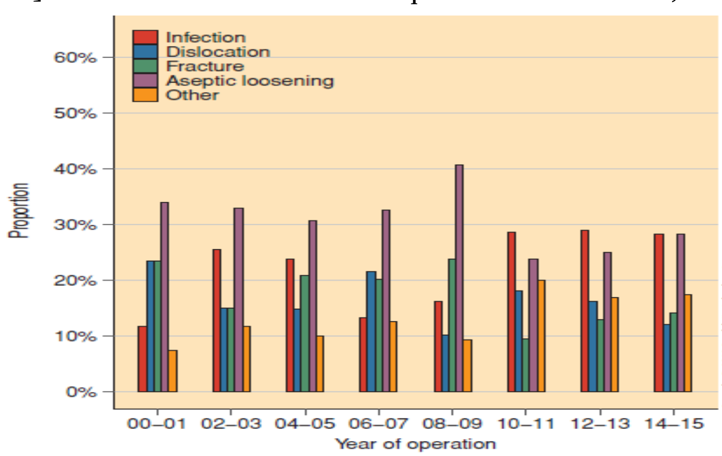

Figure 5:Probability of aseptic loosening failure as a function of time

fixation over time, or biologic loss of fixation caused by particle-induced osteolysis around the implant. This can result in implant failure.

1.3 Objectives

The objective of our research project is to reduce the modulus of elasticity of Titanium based implants. The reduction in modulus of elasticity will be achieved by reduction in density of implant by introducing porosity. The route that is taken to achieve the goal is selective de-alloying. The filler is distributed homogeneously in the sample. The filler is then removed from the sample by using de-alloying agent. This removal will lead to introduction of porosity.

1.3.0 Effect of porosity

Introduction of porosity will lead to decrease in modulus of elasticity which will result in lesser stress shielding. The introduced porosity will also increase the surface area which will lead to strong bond formation resulting in optimum osseo integration.

CHAPTER 2

LITERATURE REVIEW

2.0 Introduction

Metallic implants offer the most superior set of properties for load-bearing applications and as such, are preferred for bone replacements. However, they come with their own set of drawbacks. Metals are inherently stiff materials and as such the phenomenon of stress shielding is hard to overcome. Extensive research has been done upon the subject to diminish this long-existing issue, with some level of success being achieved. Titanium, having the lowest elastic modulus, is mainly targeted for modification. Some of the basic important properties and characteristics of both the alloys are listed below. For the purpose of this project, we shall be focusing on the beta-titanium alloy system of Titanium-Molybdenum-Zirconium[15].

2.1 Chemical composition of TiMoZr

Element	Mo	Zr	O	N	C	Fe	Ti
wt %	12.05	5.3	0.08	0.01	0.012	0.038	Balance

Table 2 - Chemical Composition of biomedical TiMoZr alloy

2.2 Mechanical Properties of TiMoZr

Young's Modulus (Gpa)	Yield Strength (MPa)	Ultimate Tensile Strength (MPa)	Elongation (%)	Hardness (HV)
90.9±2.2	956±23	1028±16	4.1±0.2	396±13

Table 3 - Mechanical Properties of biomedical TiMoZr alloy

2.3 Phases present in the alloy system

Depending on the phases present in the alloy system, titanium alloys may be α+β type or β type. Pure titanium is also employed.

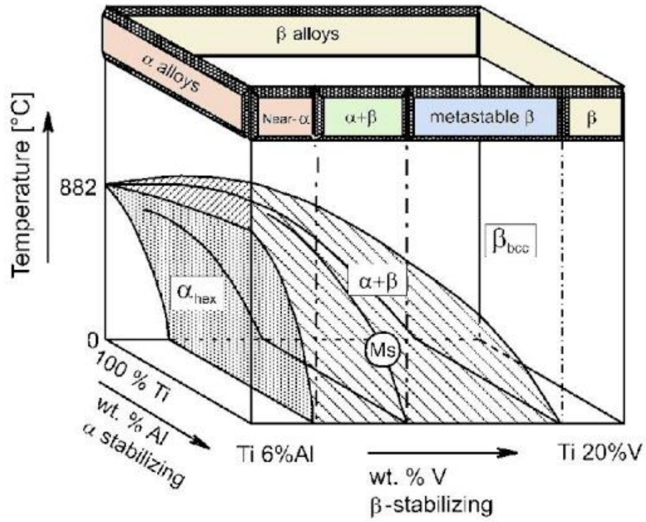

Figure 6 - Types of phases in Ti-6Al-4V system

2.3.0 Pure Titanium

The use of cp commercially pure titanium is restricted to dental implants because of its low-moderate mechanical properties. In cases where good mechanical characteristics are required for load bearing sites such as in hip implants, knee implants, bone screws, and plates, titanium alloys are mostly used.

2.3.1 α and near- α type

These alloy systems consist of α phase stabilizers such as aluminum, oxygen, nitrogen or carbon. They exhibit excellent corrosion resistance but have narrow range of low temperature strength and as such find little use in the medical industry.

2.3.2 α+β type

The α+β type alloys, such as Ti-6Al-4V, have been widely used due to a combination of mechanical and biological properties, such as high specific strength, corrosion resistance and biocompatibility. They find uses in dental and orthopedic implants and are often preferred over the other two FDA approved metallic alloys i.e. stainless steel and Co-alloy system, mainly due to their comparatively lower young's modulus. However, there is still an issue to address with the toxicity that the alloying elements impose, once placed within the body. It has been reported that Vanadium (V) may enter human tissue cells and work to disrupt enzyme activity, associated with inflammatory response of the human body. It has also been proved that the presence of Aluminum (Al) in the body makes individuals more susceptible to the development of Alzheimer's disease. Additionally, even though the young's modulus is lower than that of stainless steel and Co-Cr-Mo alloys, it is still quite higher than that of the natural bone (10-40GPa) and can cause substantial bone resorption at the site of implantation. This high modulus is attributed in part to the large amount of Aluminum present which yields high volume of α phase within the alloy. For long term implantation, these risks are unavoidable. As such, efforts are being made to move away from Ti-6Al-6V alloy system by replacing the present alloying elements with safer options.

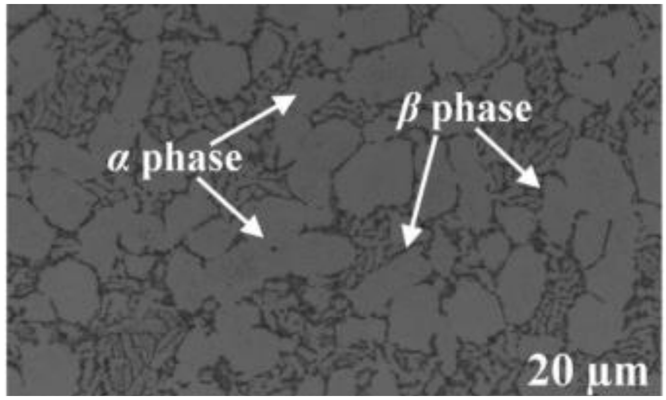

Figure 7 - Types of phases in Ti-6Al-4V system

2.3.3 β type

There is growing interest in titanium alloy systems with β or near- β phase present. Such alloying elements consist of Nb, Zr, Ta, Mo, Sn etc. the alloy systems may be binary, ternary or quaternary and examples are listed below: -

Binary Alloy Systems	Ternary Alloy Systems	Quaternary Alloy Systems
Ti-Nb, Ti-Mo, Ti-Ta, Ti-Zr, Ti-Mn, Ti–Cr	Ti-Nb-Mo, Ti-Nb-Pd, Ti-Nb-Zr, Ti-Nb-Sn, Ti-Nb-Ta, Ti-Nb-Fe, Ti-Mo-Zr, Ti-Mo-Nb, Ti-Cr-Al, Ti–Cr–Nb, Ti-Cr-Sn, Ti–Mn–Al, Ti-Ta-Nb, Ti-Ta-Sn, Ti-Ta-Zr, Ti–Mn–Fe, Ti–Sn–Cr	Ti-Ta-Sn-Zr, Ti-Nb-Zr-Sn, Ti-Nb-Zr-Fe, Ti-Nb-Ta-Zr , Ti-Mo-Zr-Fe, Ti-Fe-Ta-Zr, Ti-Cr-Mn-Sn, other systems are still evolving.

Table 4 - β-type alloy systems

The presence of β phase (or the absence of α phase) yields a structure that is more biocorrosion resistant due to adherent oxide film formation, has better mechanical properties and produces no adverse effects within the body. Most importantly it possesses a much lower young's modulus which means stress shielding is greatly minimized.

Ti-12Mo-6Zr ternary alloy system consists of purely β phase and has a young's modulus of 64GPa. It also exhibits better biocompatibility than most other alloys and as such, has much potential to replace all other metallic implants[9].

2.4 Synthesis Routes

Various methods for alloy synthesis have been explored and researched, starting from the conventional arc melting to the more advanced laser melting techniques.

2.4.0 Vaccum Arc Remelting

Vacuum arc remelting comprises of the continuous melting of a consumable electrode by means of an arc surrounded by a high vacuum atmosphere. The arc is powered by a DC power source and is directed from the electrode to the base of the mold on which deposition is to occur when electrode melts as a result of heat from the arc. The mold, often made of copper, is continuously cooled by means of water-carrying coils.

For the VAR process of titanium, the following advantages can be achieved:

(a) desorption of dissolved gasses, e.g. hydrogen and nitrogen;

(b) minimum wt % of impurity elements at high vapor pressures;

(c) oxide removal which improves cleanliness of sample produced;

(d) possibility of directional solidification of the ingot from bottom to top which homogenizes sample.

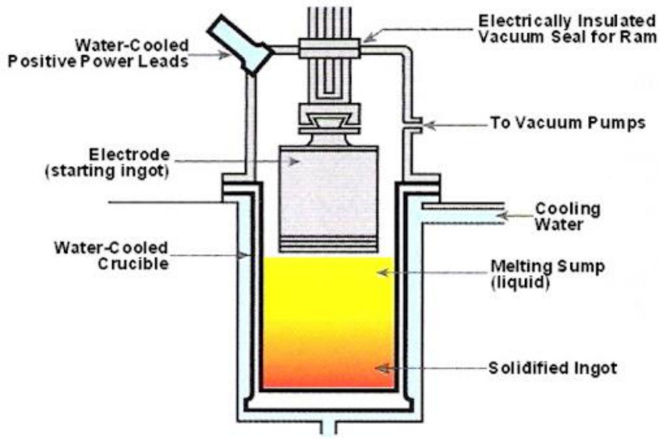

Figure 8 - VAR schematic diagram

However, the possibility of defects such as tree ring patterns, freckles, white spots and porosities, overshadow the advantage of even directional solidification[13].

2.4.1 Electron Beam Melting

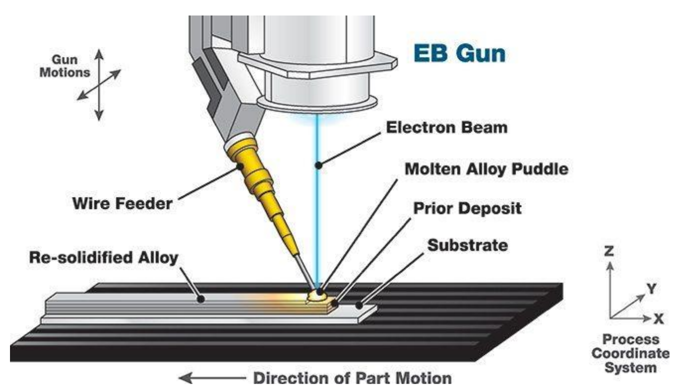

Figure 9 - EBM process schematic diagram

Reactive metals such as titanium, can be produced by the process of electron beam melting. Electron beam melting can be made economically feasible by producing large castings, preferably when the whole alloy composition range can be used. Since biomedical titanium alloys consist of a fixed composition, this method is more or less not possible. However, it should be noted that the produced castings are of superior quality than either VAR or plasma arc melting processes. Alloying elements having high vapor pressures are difficult to distribute evenly across alloy sample.

The characteristics of EB melting are:

(a) high degree of control available on parameters such as temperature, speed and reaction type;

(b) possibility to choose from wide range of raw materials[13].

2.4.2 Plasma Arc Melting

Plasma arc melting (PAM) is a material processing technique in which the thermal heat of the plasma is used to melt feed material. PAM furnaces are operated under slightly positive pressures to prevent the potential atmospheric contamination or selective evaporation of alloying elements. PAM can be used in place of VAR or EB casting when the limitations of those processes hard to overcome.

The disadvantages of VAR that may be experienced are:

(a) less control of heating rate i.e. superheating;

(b) the electrode used is quite expensive and of low quality[13].

2.4.3 Vaccum Induction Melting

When complex shapes must be made or one is dealing with reactive metals such as Titanium, Vacuum induction melting (VIM) may be employed. High degree of homogenity is attained by the electromagnetic agitation which results in even distribution of elements. Measures are undertaken to reduce contamination via graphite crucible by preheating it in vaccum[13].

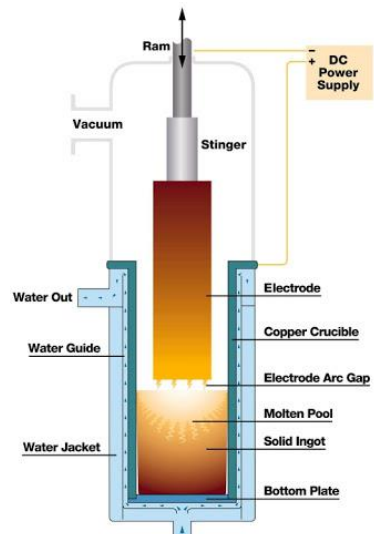

Figure 10 - VIM process schematic diagram

2.4.4 Powder Metallurgy

In areas where fine grained microstructures and superior physical properties are required, it is beneficial to undertake the powder metallurgy route. It can be coupled with computerized softwares, which allow for easy customization of parts.

Advantages of this process are:

a) short production cycles

b) composite materials or porous materials can be produced

Final properties of compact depend on the PM route taken for eg.

- press and sinter technique results in porous compacts while degrades properties;
- hot pressing (HP) and hot isostatic pressing (HIP) have reduced porosity, and conversely higher stiffness[13].

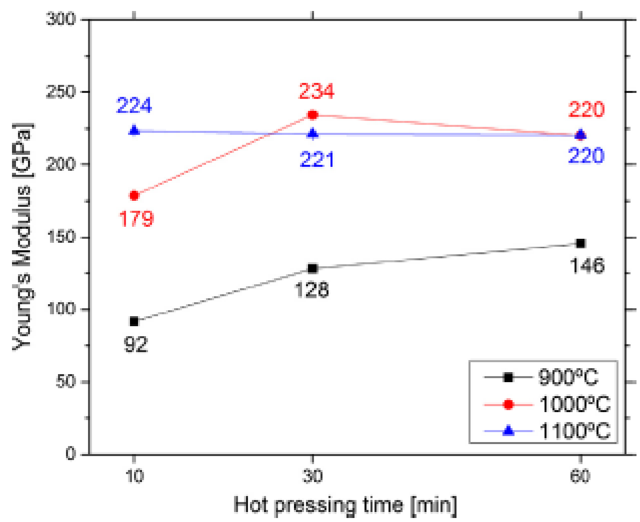

Figure 11 - Young's Moduli of CoCrMo compacts hot-pressed at different

2.5 Metallic foam

Porous materials are materials having large amounts of porosity. Porous metals or metallic foams have some exceptional characteristics such as enhanced mechanical properties, low density, large specific area, good energy absorption, greater strength and reduced stiffness when compared with bulk metals. In addition to

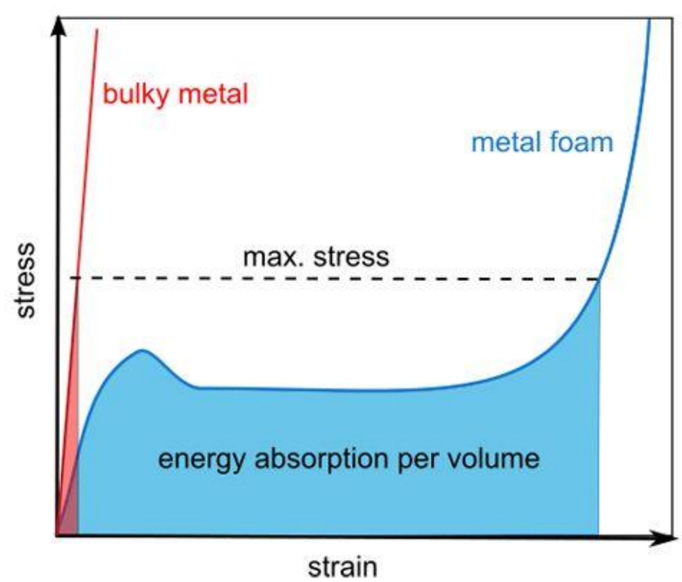

Figure 12 - Stess-strain curve of metal foam vs bulk metal

previously mentioned features, metal foams also offer electrical and thermal conductivity, ease in loading and unloading, high and low temperature tolerance, thermal shocking resistance and toughness. Due to these enhanced properties of the metal foams, they are made into filters, fluid separators, heat exchangers, heat radiators, flame retarders, mufflers, damper buffers, porous electrodes, catalysts and their carriers, human implants, electromagnetic shields, light structural parts for aerospace industry. Their wide range of applications, from structural to functional, are influenced by type of porosity i.e. open or closed.

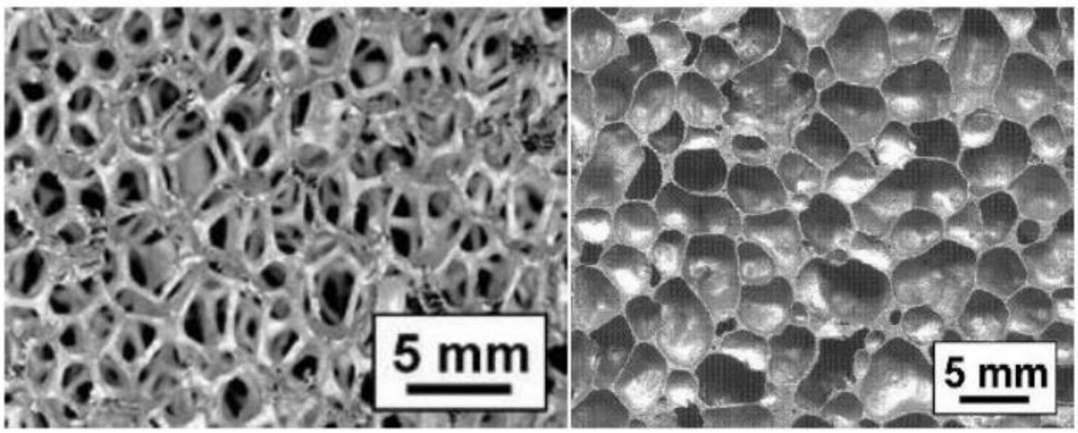

Figure 13 - Open porosity (left) and closed porosity (right)

Closed foams consist of pores that can be sealed while in open foams, the pores are interconnected and form a continuous network throughout the metal. As such, the open cell foams are generally less stiff than closed cell foams.

Foams with open structure can meet both load bearing and functional requirements whereas closed foam fulfill the demand of structural applications only.

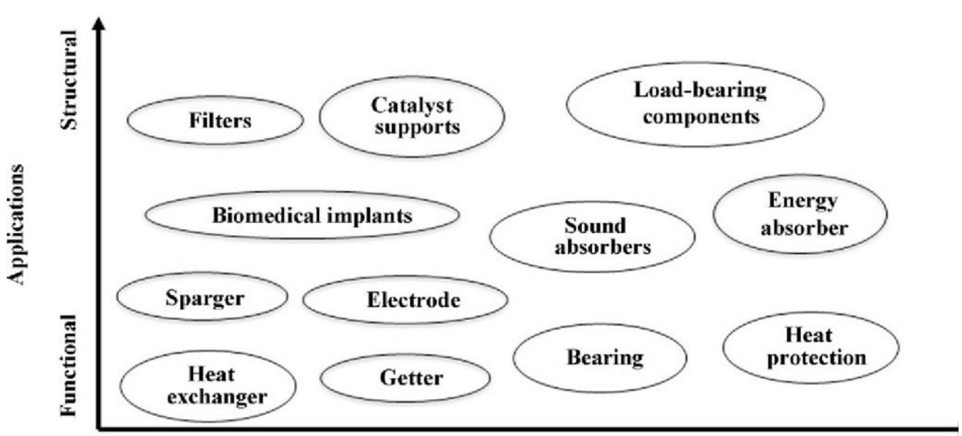

Figure 14 - Applications of open and closed metallic foam

The usage of foams with open network in biomedical applications is because of the interconnectivity of the pores and the resulting mechanical properties they offer. The interconnection between pores helps in the movement of various body fluids and provides increased number of attachment sites for bone cells, while their mechanical properties lessen stress shielding phenomena. Thus, metallic foams provide a unique combination between biocompatibility and strength so that they can be used in number of biomedical applications such as dental implant, acetabular systems, fusion device and fixation system.

2.5.1 Mechanical Properties of metallic foams

The mechanical properties of metallic foams are dependent on their relative densities and cell wall properties. Therefore, these properties can be tailored as per the place of usage. Under compressive force, metallic foams deform in a different way from bulk metals due to their structural differences. The curves obtained during compression load, for metallic foam, reveal three different regions: initial linear elastic region, plateau region and finally densification region.

Compressive failure of foam is a continual process in which pore collapse and layer by layer fracture is observed perpendicular to the direction of applied force. As particles fill up the empty spaces formed by pores, densification starts to occur.

The curve obtained typically represents the elastic –brittle nature of the foam. The initial linear elastic region is due to the elastic bending of cell walls and the plateau region represents the brittle folding of the cell walls. Finally, the densification region signifies the filling of pore spaces and resulting increase in stress, above the elastic limit. It is also reported that the higher the value of ppi (pores per inch), the greater the quasi-elastic modulus and limit stress.

The study of initial compressive responses of an open cell and closed cell foams revealed that the slopes of loading and unloading for open cell are undistinguishable and linearly elastic while closed cells exhibit an initial linear regime at strains of up to about 0.01, the slope of the loading curve is much lower than that unloading, indicating that there is some plastic deformation, even at low strains.

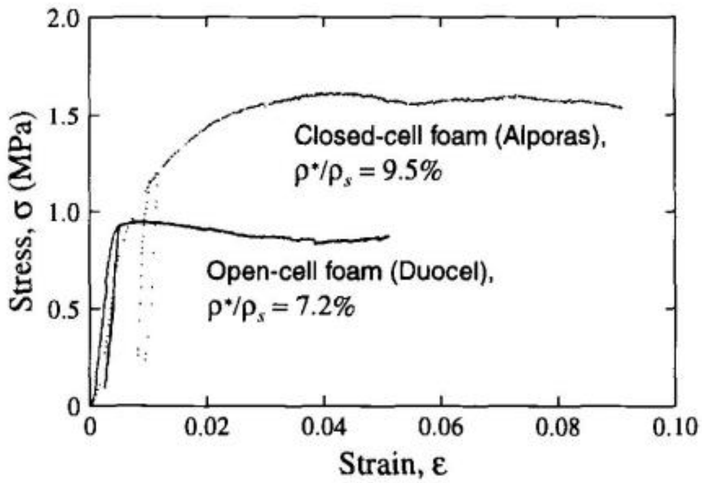

Figure 15 - Stress strain curve for open and closed-cell foams

Before approaching plateau stress, relatively homogenous deformation of open cells is observed when subjected to surface strain mapping while closed cell distorts heterogeneously, yielding locally by deformation banding at stresses about the half of the plateau stress. Closed cells materials strain increases up to the peak stress and then lowers. When tensile stress-strain curve is plotted, and studied it showed the same behavior as compression curves[20].

2.5.2 Metallic foam synthesis routes

The flow chart below lists some of the more common methods by which metallic foams have been made and their properties researched.

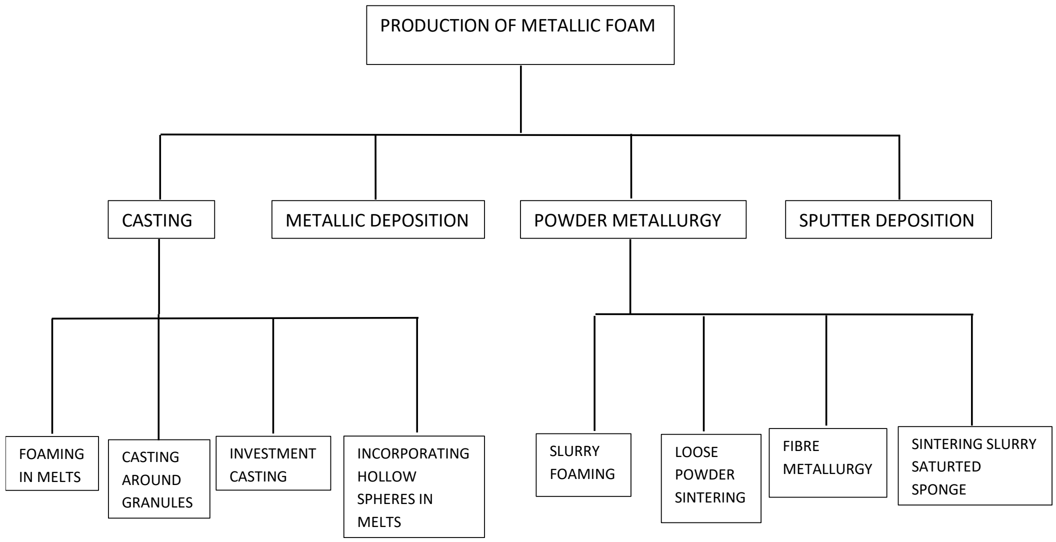

Figure 16 - Stress strain curve for open and closed-cell foams

However, some of the more novel techniques of metal foam making are discussed below:

2.5.2.0 Liquid foaming method

A novel method of metallic foam production called liquid foaming process consists of the following precursors which form a solution:

I. Carboxymethyl Cellulose Sodium (CMC) as binder
II. Sodium Hexametaphosphate (SHMP) as dispersant
III. H2O2 as foaming agent

Process consists of mixing the alloy powder in question, e.g. Ti or Co, with the solution mentioned. This produces a slurry type mixture which is agitated for approximately an hour at room temperature. This yields a homogenous slurry. The slurry mixture is then poured into a mold where it is kept at 40–60 °C for 3 hrs. The samples, now dried, are then heated to 1300 °C in vacuum environment for 3hrs for sintering to occur[16]. The results of this process on Titanium substrate are shown:

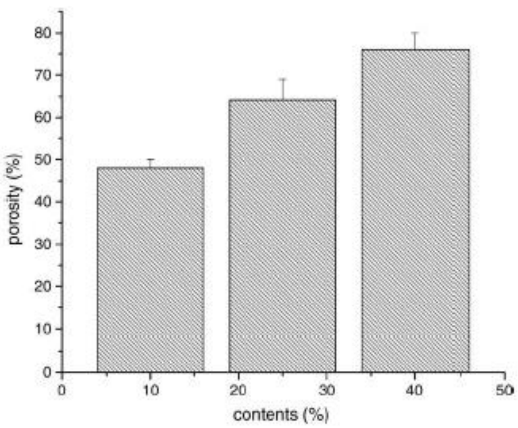

Figure 18 - Porosity of porous titanium prepared using various H202 contents

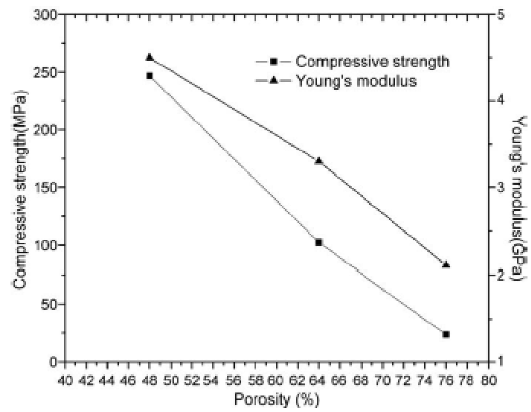

Figure 17 - The effect of porosity on the compressive strengths and young's modulus of porous titanium

2.5.2.1 Additive Manufacturing

Complex geometries can be formed via additive manufacturing which would not be possible in conventional methods of casting or forming.
The most common techniques that are being used today are selective laser melting (SLM) and electron beam melting (EBM).

SLM is carried out by a laser beam which moves on top of a metal powder bed, suspended in inert conditions.

EBM consists of an electron beam scanning the powder bed in vacuum after a fast preheating step, usually above 600-700˚C.

Since both processes consist of different cooling rates, i.e. different solidification mechanism, the resulting microstructure and properties differ substantially. As of now, most AM work is focused on processing Ti-6Al-4V alloys, and very little is done for the superior β-titanium alloys[7].

One of the simpler techniques, and worth noting, to produce metallic foams is:

2.5.2.2 Furnace sintered metal powders

This is most simple technique used for the fabrication of metallic foam. It proceeds by compacting, binding and sintering of metal powders. During sintering, high temperature is applied to bond the powder particles in a compact manner without causing any major effect on the particle geometry. A binder is added to keep the particles of the powder together which guarantees a wider area for the movement of mass between particles in the solid-state diffusion technique. Usually metallic foams of Co-Cr alloys[18], commercially pure Ti and its alloys [19] can be developed using this technique. The only limitation of this approach is that pore size and shape are defined by the attributes of powder being used.

CHAPTER 3

METHODOLOGY

3.0 Alloy synthesis and sample preparation

The titanium alloy is prepared with additions of molybdenum and zirconium as major alloying elements. The selection of molybdenum and zirconium as an alloying agent is based on the fact that they enhance the strength and corrosion resistance of Beta-Titanium. A less noble element is added to the alloy to which undergoes selective dealloying to produce a porous structure. This filler element is selected based on various factors including enthalpy of mixing, crystal structure, electronegativity difference, atomic structure. Varied amount of filler elements is added in TiMoZr alloy according to weight percentages. The weight percentages taken for study are mentioned below:

1. TiMoZr-0 weight percentage of filler element (Reference)
2. TiMoZr-5 weight percentage of filler element
3. TiMoZr-10 weight percentage of filler element
4. TiMoZr-15 weight percentage of filler element
5. TiMoZr-20 weight percentage of filler element
6. TiMoZr-25 weight percentage of filler element

3.0.1 Arc Melting

Arc furnace MAM-1 (shown in Figure 19) was utilized to synthesize the alloy. The furnace produces stable arc for melting and combining the elements. The anode is composed of graphite because of its high temperature stability and good electrical conductivity. The cathode is a copper plate including five small crucibles for alloy preparation. This copper plate is kept cool in order to avoid melting by using cooling coils running beneath the plate. Cool water runs inside the coils which comes from the chiller. Titanium, along with alloying elements and filler element, is placed in a crucible with specified weight percentages. The anode and cathode are enclosed in a glass chamber. The chamber is closed and high vacuum is created inside it using pumps usually in order of 10^-5. This vacuum helps to remove any reactive element or gas such as oxygen from the chamber. Non-reactive gas, usually argon, is purged inside the chamber to provide an inert environment and maintain cleanliness. The anode is focused on the crucible, using a controlling handle, and arc is produced by providing electric current. The temperature of the arc is directly related to the provided electric current and it can reach up to 3000℃.

Figure 19 - Arc Furnace MAM-1

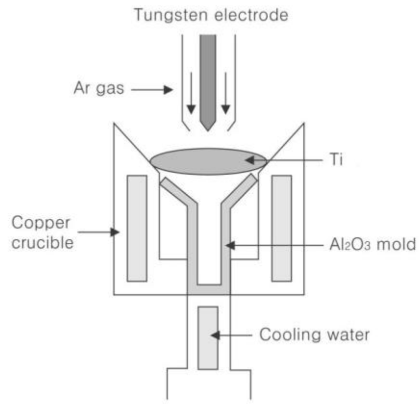

Figure 20 - Schematic of Vacuum Arc Melting

The produced arc completely melts and combines the elements homogenously. The arc should not be kept above the alloy for a longer period of time, as it can vaporize alloying elements which will change the alloy's composition. Figure 20 shows schematic of typical arc furnace.[13]

3.0.2 Electric Spark Wire Cutting

The samples were cut in small sections using EDM wire cutting machine. This technique allows machining of small workpieces that are prone to damage if conventional cutting methods were to be adopted. These samples then undergo de-alloying. Figure 21 shows schematic of EDM wire cutting machine.

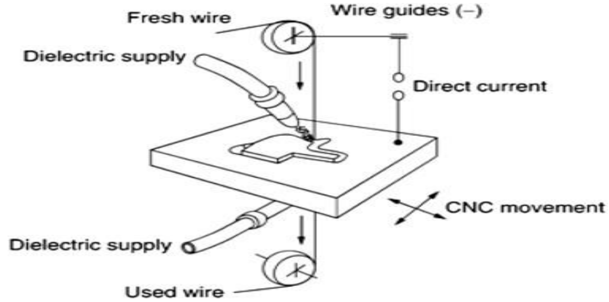

Figure 21 - Schematic of EDM Wire cutting machine

3.0.3 Surface preparation for Metallographic Characterization

A polished and plane surface is required for getting optimum characterization results. This process is known as metallographic sample preparation. The samples were mounted in bakelite using hot compression mounting machine. After mounting, the scratches of sample surface were removed by grinding on grinding wheel.

Silicon-Carbide (SiC) paper ranging from 120 to 2000 grit size were used. The grinding process starts from grinding on coarser paper and then moving towards finer grit size. After grinding on 2000 grit size, majority of scratches are removed with presence of very small fine sized scratches. These scratches are removed by polishing the samples, which is the last step of sample preparation.

To get smooth surface, polishing is done on polishing wheel which has a very fine polishing cloth on rotating wheel. Polishing suspension, containing alumina round particles ranging from particle size 1 µm and 0.5µm, was used. Sample was polished by applying the suspension on rotating polishing cloth and pressing the sample against the wheel. This resulted in a shiny finished surface with no presence of any scratches.

The finished surface was then cleaned with ethanol and de-ionized water.

3.0.4 Chemical Dissolution of filler element

The process of de-alloying is done by chemical dissolution using an appropriate dealloying agent. The filler element is selectively dissolved by the dealloying agent through diffusion process, without degrading the main β-titanium alloy matrix. The dissolution of filler element inside the alloy system is a function of concentration of agent, time given for de-alloying and the weight percentage of filler element inside the alloy system. The alloy samples were dipped inside the de-alloying solution for total of 24 hours with intervals of 1 hour to record the weight loss as a function of time. After each hour, the sample were taken out of the de-alloying solution. Then, the sample were washed in distilled water using sonication for about 15 minutes to make sure the complete removal of de-alloying solution. After the samples were washed, the samples were heated on hot plate at 120-150˚C for about 30 minutes in order to make sure that all water is evaporated. After all these steps, the weight loss measurements were recorded. This process helped in attaining porous TiMoZr alloy system.

3.1 Characterization Techniques

Different characterization techniques were utilized to study the effects of de-alloying experiments and subsequent formation of porous structure in samples. The morphological and microstructural study of reference and de-alloyed TiMoZr system was carried out using Scanning Electron Microscopy. X-Ray Diffraction analysis was carried out for studying crystal structure and elements present inside the system. Both of these techniques were utilized before and after de-alloying process.

3.1.0 Scanning Electron Microscopy (SEM)

Scanning electron microscopy is used a microscopy technique which utilize electron beam instead of visible light. As the wavelength of electron beam is smaller than that of light (380 to 700nm), SEM provides superior magnification and resolution (better than 1nm) compared to visible light based (optical) microscopes. Scanning electron microscopy is performed by bringing the polished specimen in contact with the electron beam. A strong electron beam of specified energy is produced by an electron gun powered by thermionic or field emission. Electron beam utilize raster scanning to focus on rectangular area of specimen using magnetic condensers. This electron beam interacts with the surface of material and depending upon the material it undergoes refraction, diffraction and reflection along with giving secondary electrons, backscattered electrons, photons etc. These resulting beams (signals) are detected by an array of detectors in the microscope. The data collected from detectors array gives of the final image using software. Amplified signals produce a magnified gray scale image of the sample’s surface with extremely high resolutions in the nanometer range. The difference between electron densities of the element give varied number of signals from the surface and denser signals appear to be brighter part in the image. Depending upon the number of electrons emitted, high atomic number elements appear as brighter and low atomic number element appear as relatively darker[21]. A schematic of typical SEM is shown in Figure 22.

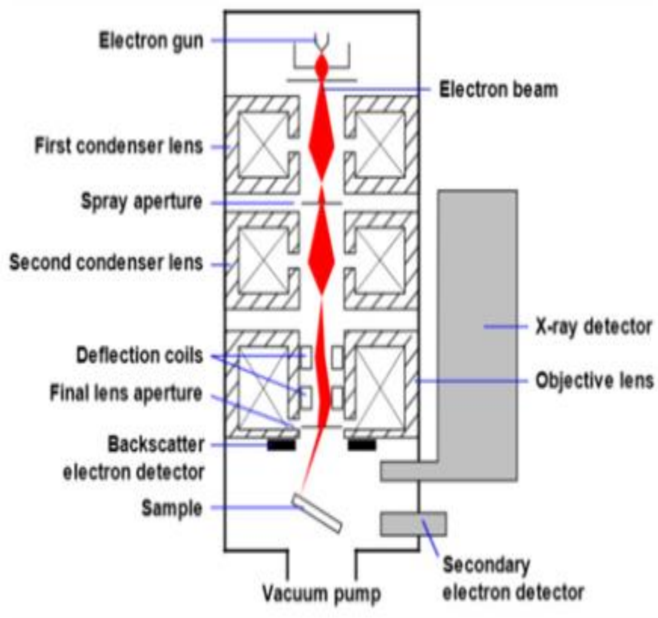

Figure 22 - Schematic of SEM

The SEM analysis can carry out following analysis

- Identification of metals and materials
- Classification of materials (microstructural analysis)
- Detection of Phases present
- Product and process failure and defect analysis
- Examination of surface morphology (including stereo imaging)
- Analysis and identification of surface and airborne contamination
- Topographical analysis
- Biological analysis

3.1.0.0 Modes utilized

In present study, SEM technique was used for following analysis

- Microstructural analysis
- Analysis of porosity

In present work, JSM 6490LA SEM present at SCME, NUST was used to carry out this analysis. The secondary electron imaging mode was used to produce images of different magnifications. Operating voltage of 5-20KV was applied with working distance of approx. 10mm. Figure 23 shows the JSM 6490LA SEM at SCME that was utilized for this project

Figure 23 - Scanning Electron Microscope- JSM640LA

3.1.1 X-Ray Diffraction Analysis (XRD)

X-Ray Diffraction analysis is used for determination of crystal structure and lattice parameters of crystalline materials. Figure 24 shows the schematic of X-ray Diffraction The working principal of XRD analysis is based on constructive interference of monochromatic X-rays diffracted from crystal planes of sample that is to be analyzed. These X-rays are generated using cathode ray tube (CRT). This produced X-ray beam is polychromatic. For accurate results, monochromatic X-ray beam is preferred. So, the produced X-ray beam pass through a filter to only give off monochromatic characteristic X-ray beam. This beam is collimated to concentrate and directed towards the sample. When these X-rays strike the sample with specific angle of incidence. Diffraction occurs from atomic layers of sample. These diffracted X-rays undergo destructive and constructive interference. After diffraction, the out of phase X-rays that show destructive interference cancels each other out and do not contribute in providing any meaningful data. However, remaining X-rays shows constructive interference due to in phase diffraction. This phenomenon of interference depends upon the distance between the parallel crystal planes in material which is different for different materials due to variation in atomic sizes forming the crystal lattice. The constructive waves satisfy Bragg's law. This law relates the electromagnetic radiations wavelength to the diffraction angle and the lattice spacing in a crystalline lattice[22]. It is written as:

$$2d\sin\theta = n\lambda$$

Where,

d = inter planar space

θ= angle of diffraction

λ = X-ray wavelength

n= order of diffraction

This results in production of intense signal that is detected and recorded by detector. A graph is then plotted between 2θ on X-axis vs Intensity on Y-axis from given data of detectors. This diffraction pattern generated by XRD analysis represents a unique crystal structure present in the sample. Upon proper interpretation and comparison of data with standard reference patterns and measurements, the results provide identification of crystalline forms in samples.

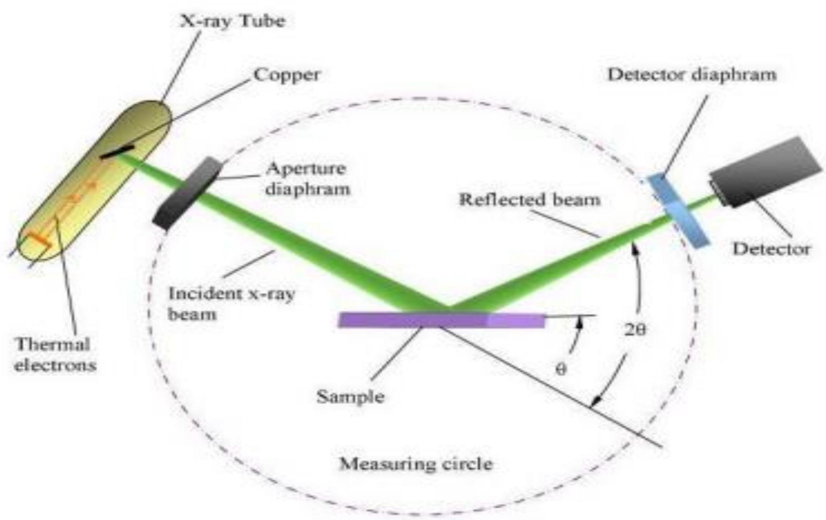

Figure 24 - Schematic of XRD Apparatus

In this present analysis, X-rays were generated by using copper anode source. These X-rays were K-Alpha characteristics x-rays with carrier energy of 1.54KeV passed through Nickel filter to produce a diffraction pattern over the sample with scan angle ranging from 20- 80^o. The scan time for each TiMoZr sample was 90 minutes. STOE $\theta - \theta$ X-ray diffractometer (Shown in Figure 25) which is present at SCME was utilized for this analysis. X'pert High Score Plus software was used to identify phases present in prepared alloy and removal of filler element after de-alloying. The analysis was done before and after de-alloying procedure.

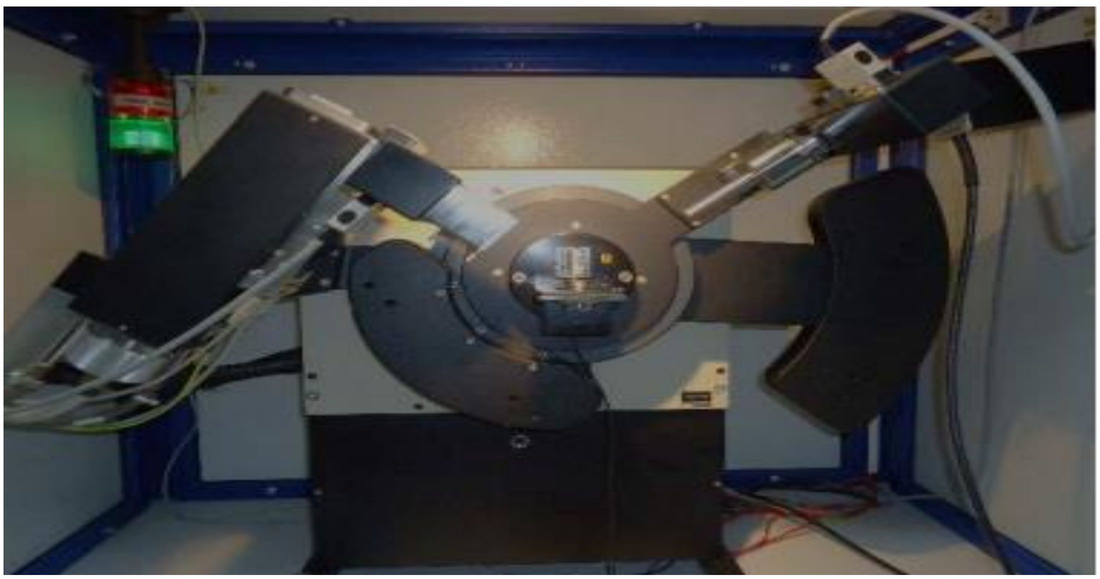

Figure 25 - STOE θ-θ X-ray Diffractometer

CHAPTER 4

RESULTS AND DISCUSSION

This chapter comprises of detailed discussion of the results that were obtained by various experimentation and characterization techniques. Synthesis of TiMoZr porous alloy system with varying amount of percentage porosity will be part of this chapter. The characterization techniques that shows the positive results of experimentations are discussed in subsequent portions of this chapter.

4.0 Development of TiMoZr porous alloy

Synthesis of TiMoZr alloy with varying amount of filler element was first achieved via melting route. Arc melting was used to melt the alloy and filler to form a solid solution and subsequent cooling resulted in a homogenously distributed filler element in TiMoZr matrix. The enthalpy of mixing of this combination is found to be slightly positive which allows atoms to mix initially and form a solid solution. However, upon cooling, the TiMoZr matrix starts rejecting the filler element into its surroundings. This results in homogenous distribution of pure filler element in TiMoZr alloy matrix along the grain boundaries. The weight percentage of filler elements in TiMoZr alloy is varying from 5% to 25% in samples. It gives of varying amount of introduced porosity upon removal of filler element in de-alloying solution.

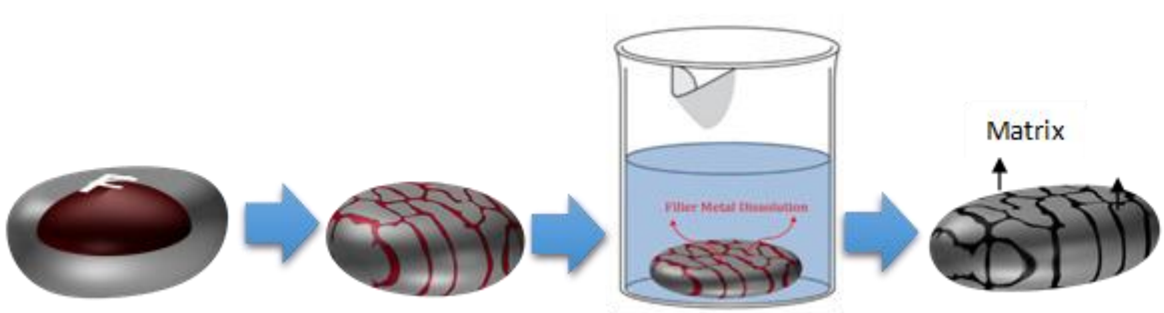

Figure 26 - Schematic of development of TiMoZr porous alloy

The table given below gives profile of weight loss percentage with respect to time

		Weight Loss (%) for Each Composition				
		5%	**10%**	**15%**	**20%**	**25%**
Time duration of dipping (hrs)	**1**	0.43	1.65	2.81	4.07	6.52
	2	0.688	2.56	5.15	6.23	9.94
	3	0.893	3.27	6.76	8.22	13.0
	4	1.10	3.73	8.08	9.61	14.82
	5	1.26	4.24	9.26	10.29	16.69
	10	1.99	6.36	13.57	15.73	23.58
	20	2.96	9.16	18.72	21.39	34.84
	24	3.56	10.23	20.13	22.93	36.82

Table 5 - Weight loss percentage relation with time

This data gained from experiments is plotted in form of scatter graphs and bar chart to give a graphical representation of dealloying progress.

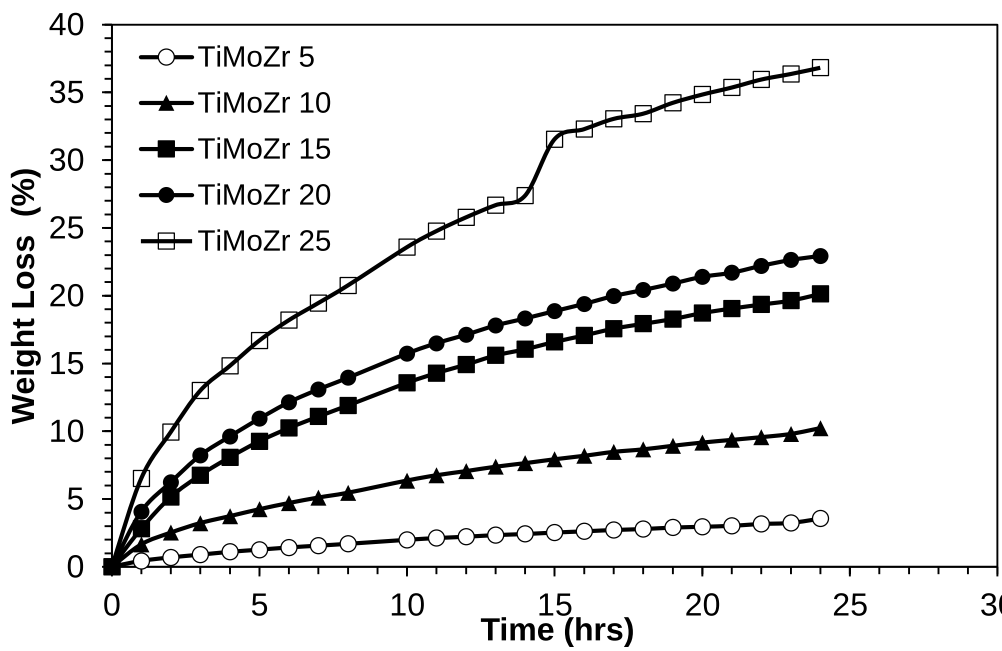

Figure 27 - Weight loss percentage w.r.t time

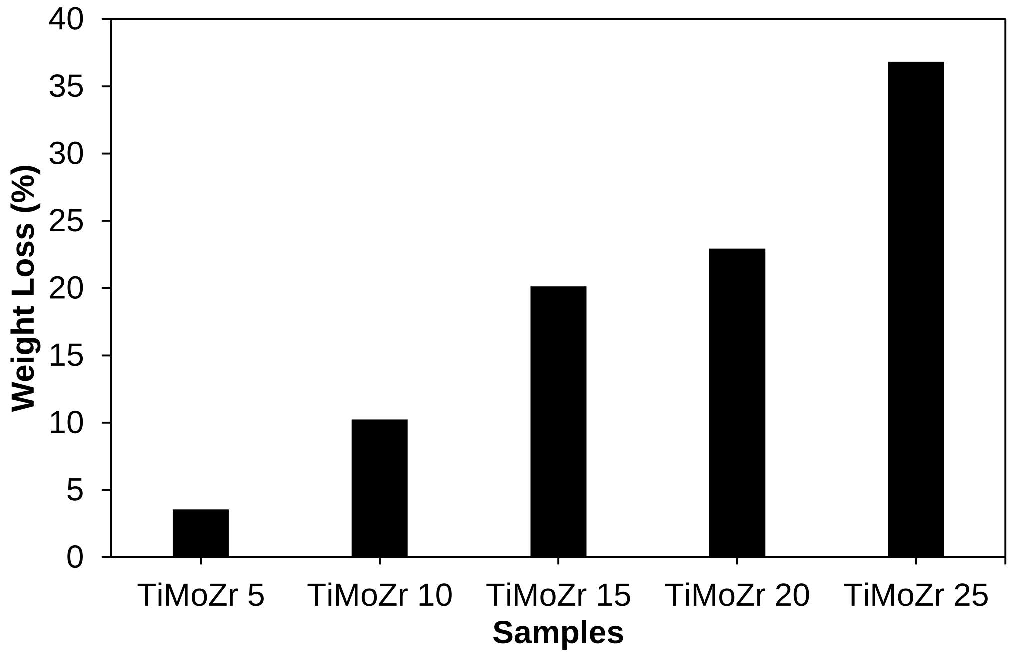

Figure 28 - Bar chart showing percentage weight loss of each sample

These total weight loss calculations resemble with the weight of the filler element added at the beginning which means that filler element is completely removed leaving behind porous structure. The level of porosity generated in each composition is equal to the added amount of filler element.

4.1 SEM Analysis

In the previous topic, we saw that the filler element was removed after de-alloying by percentage weight loss analysis. However, there is a need to make sure the filler distributed homogenously throughout, and thus resulted in a three-dimensional interconnected porous system after de-alloying. Therefore, scanning electron microscopy analysis was done to study the microstructure of TiMoZr alloy before and after de-alloying.

4.1.0 Before De-alloying

Before de-alloying SEM images show homogenous distribution of filler element. The filler element are the black spots within the TiMoZr matrix, which is the major area seen in the images. The amount of filler element is increasing with increasing weight percentage of filler element i.e from TiMoZr 5 to TiMoZr 25.

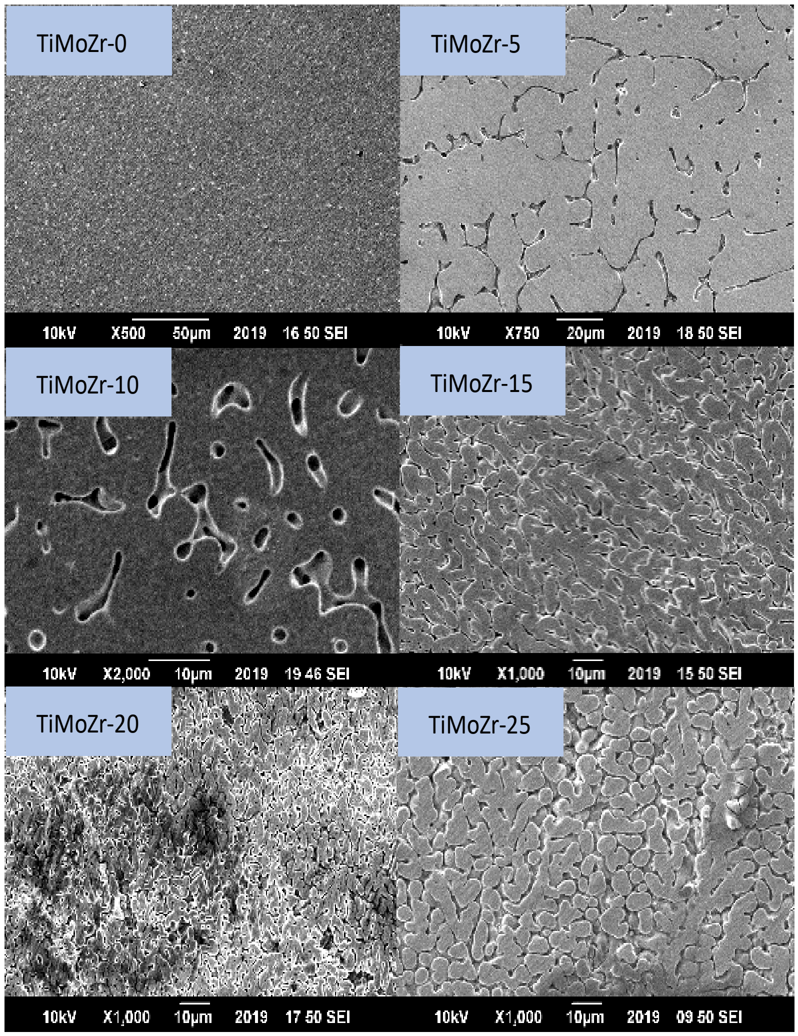

Figure 29 - SEM images of as it is samples

4.1.1 After de-alloying

The SEM images of de-alloyed samples shows the removal of filler element. This removal of filler element introduce porosity. The porosity can be seen as light spots which have replaced the previously present black spots. Likewise, the porosity is increasing with increasing percentage of filler element.

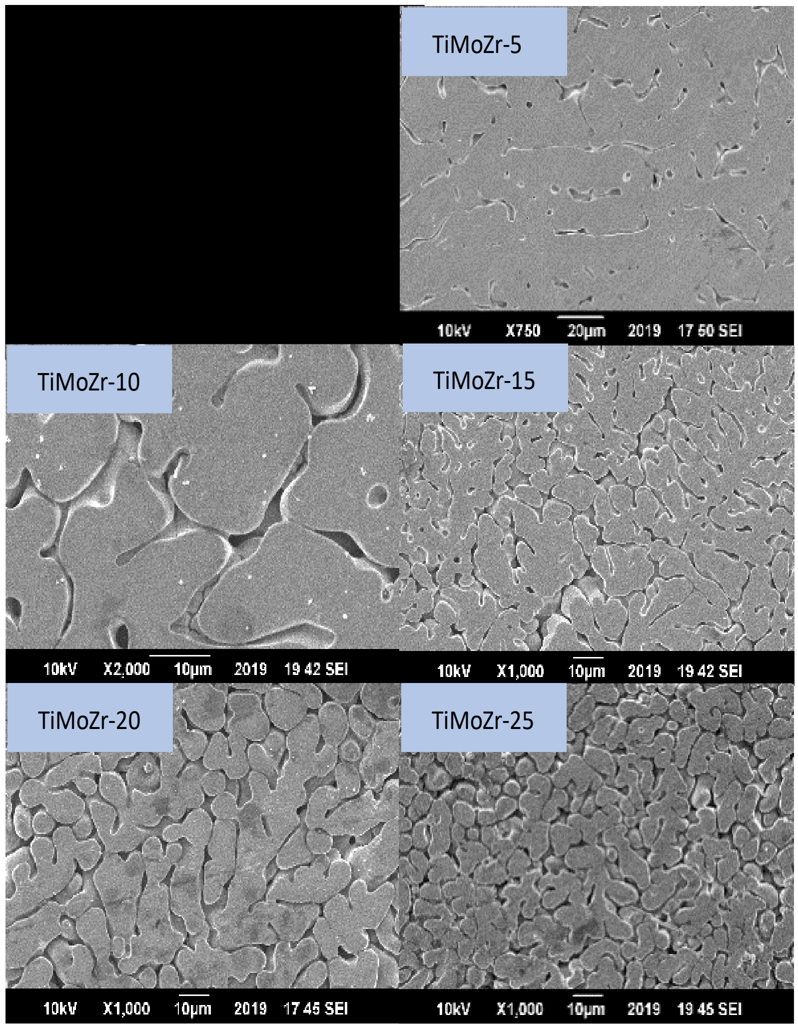

Figure 30 - SEM images of dealloyed samples

4.2 X-Ray Diffraction Analysis

XRD analysis was done to check the complete removal of filler element after de-alloying. The Analysis was done before and after de-alloying. The XRD analysis results are shown below.

TiMoZr-0

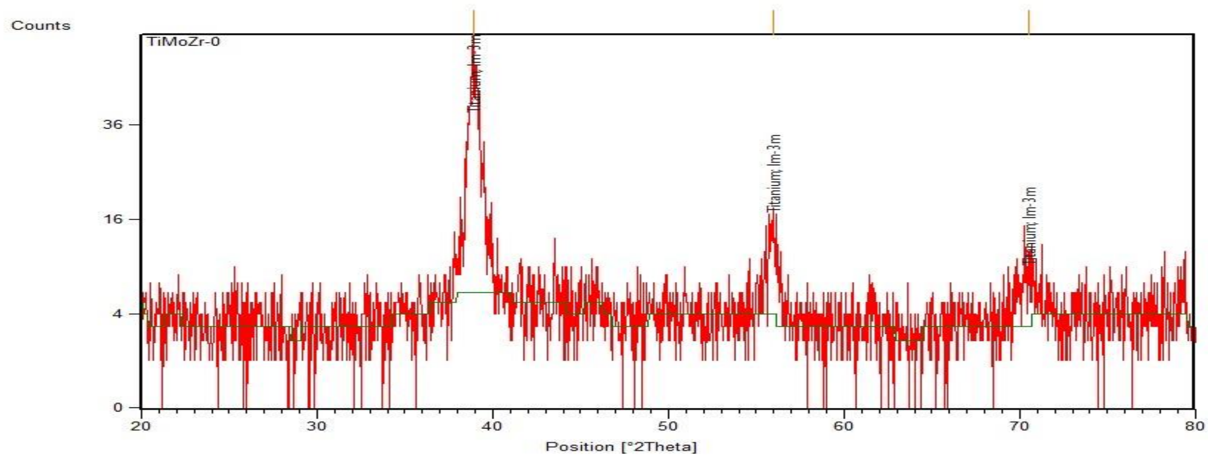

Figure 32 – Before dealloying XRD : TiMoZr 0

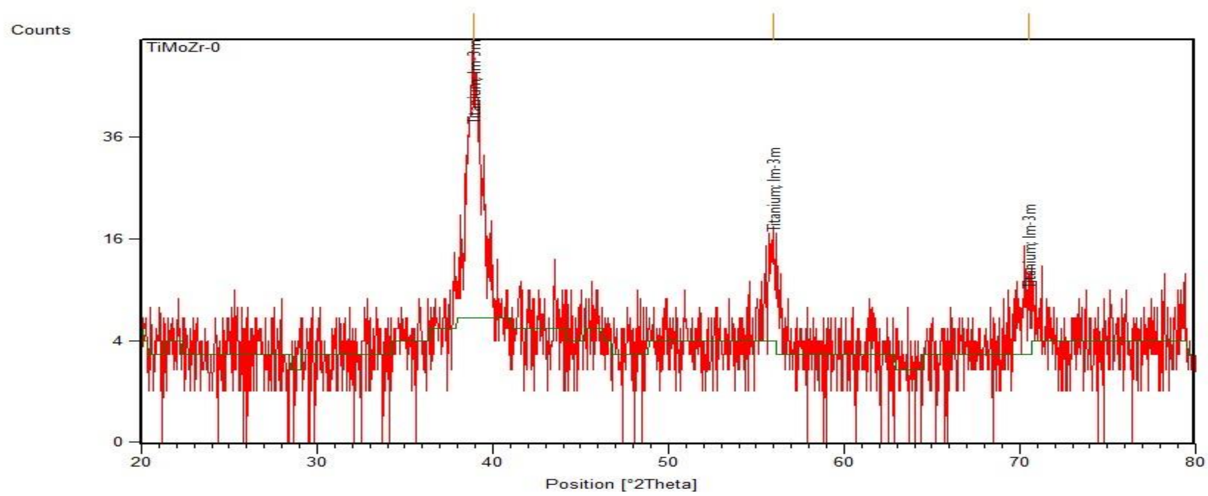

Figure 31 – After dealloying XRD : TiMoZr 0

TiMoZr-5

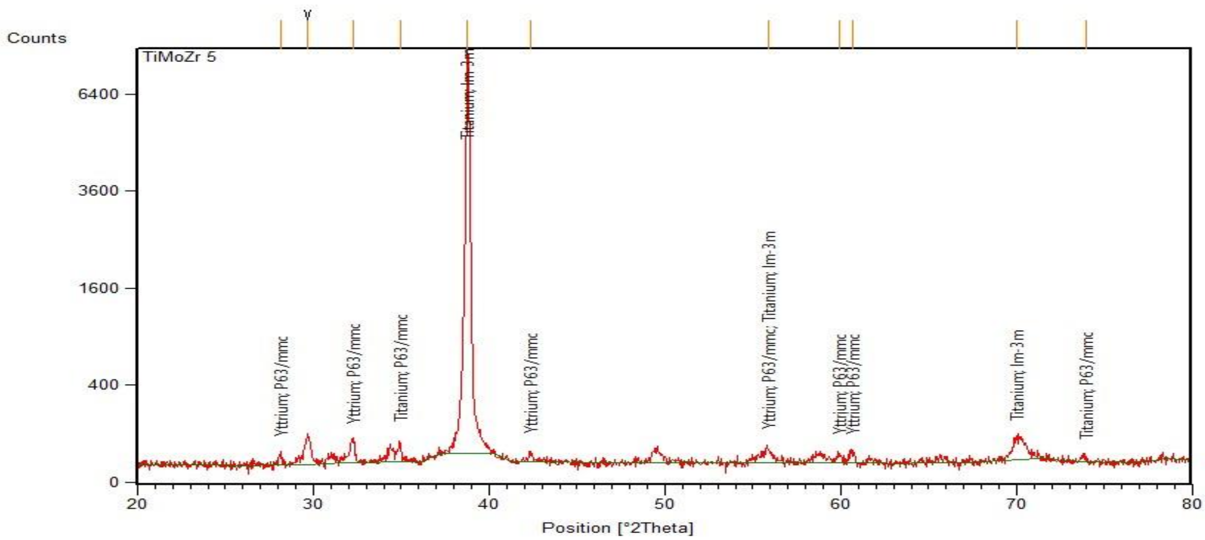

Figure 33 - Before dealloying XRD : TiMoZr 5

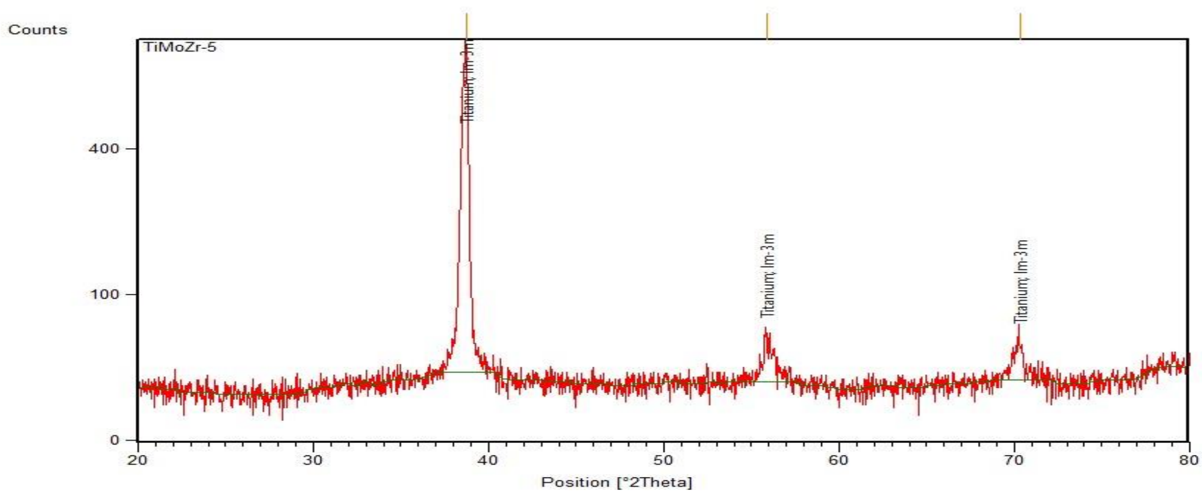

Figure 34 - After dealloying XRD : TiMoZr 5

TiMoZr-10

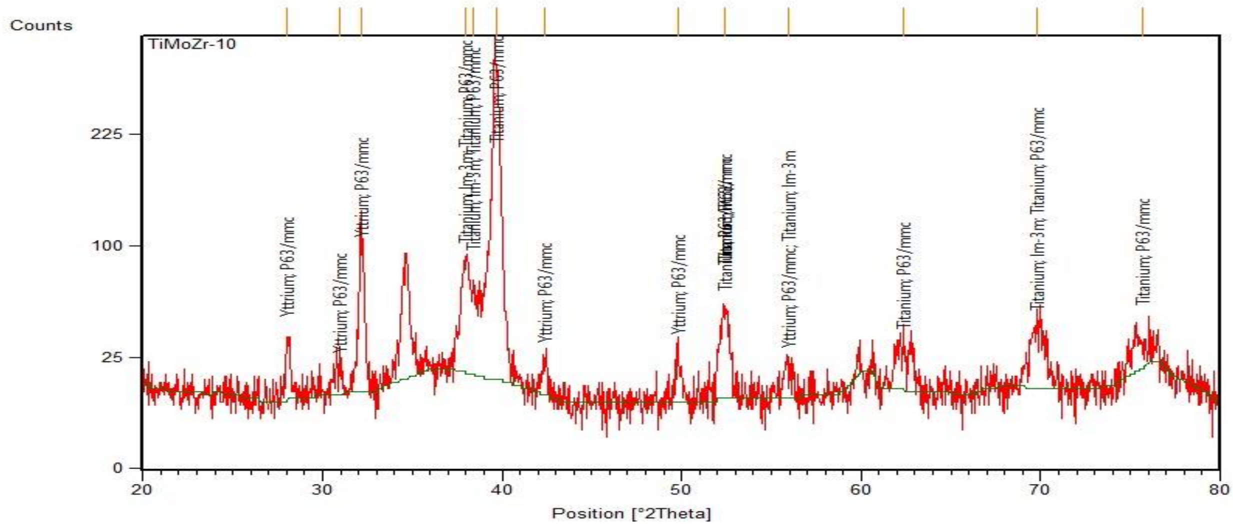

Figure 35 - After dealloying XRD : TiMoZr 10

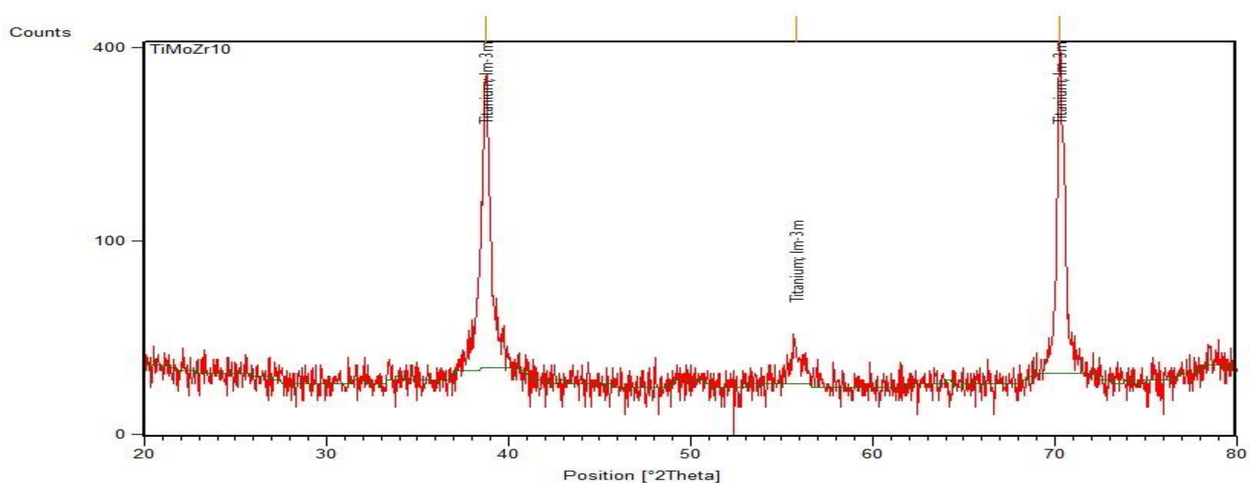

Figure 36 - Before dealloying XRD : TiMoZr 10

TiMoZr-15

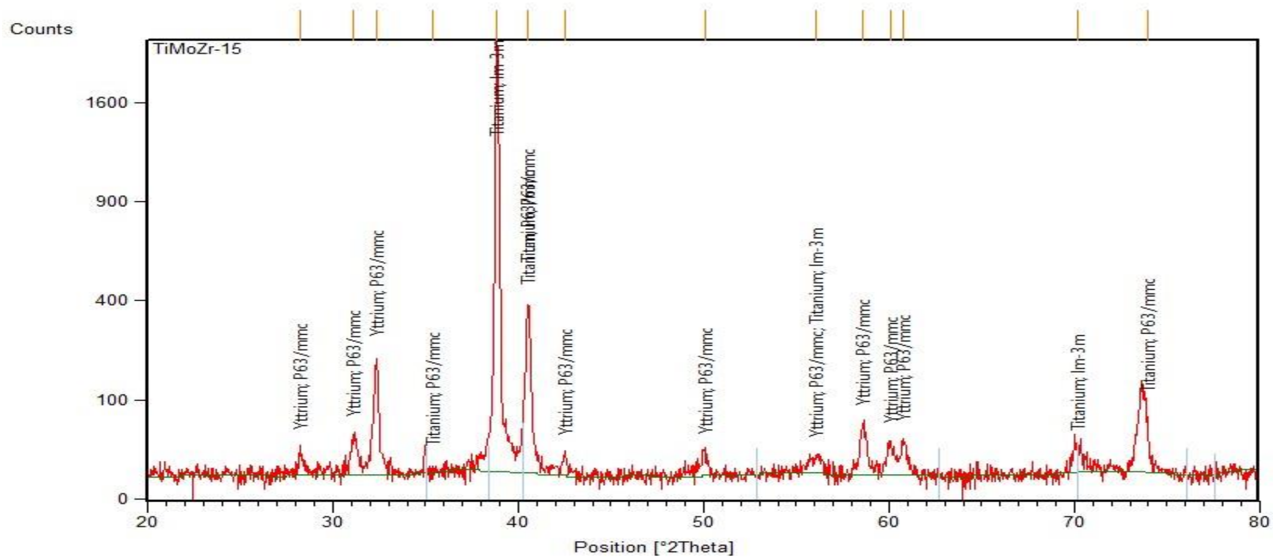

Figure 38 - Before dealloying XRD : TiMoZr 15

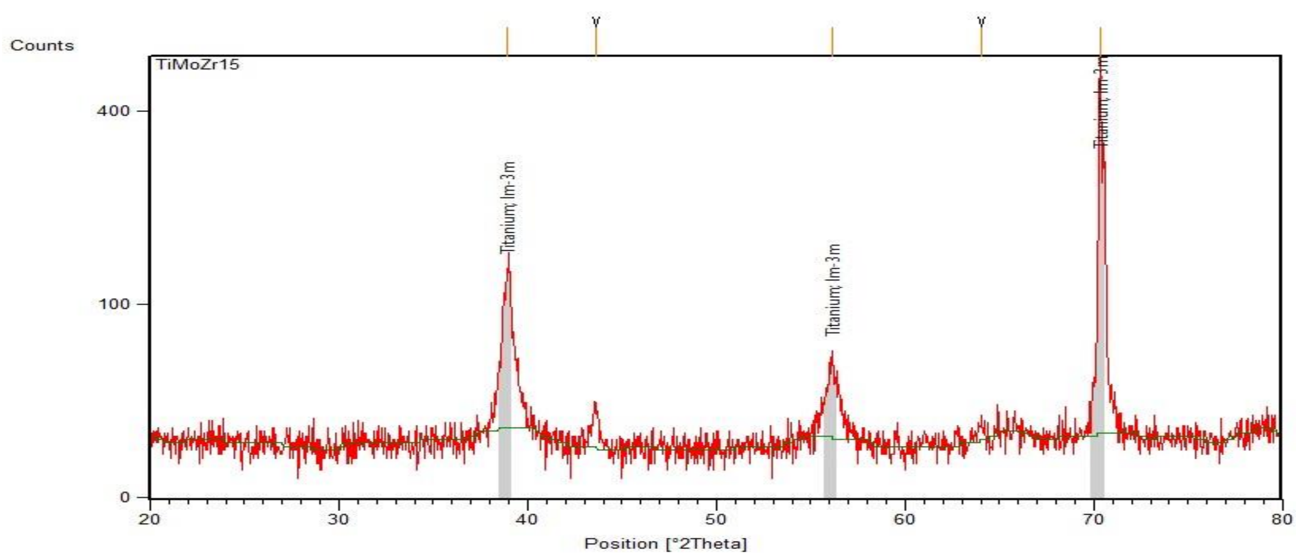

Figure 37 – After dealloying XRD : TiMoZr 15

TiMoZr-20

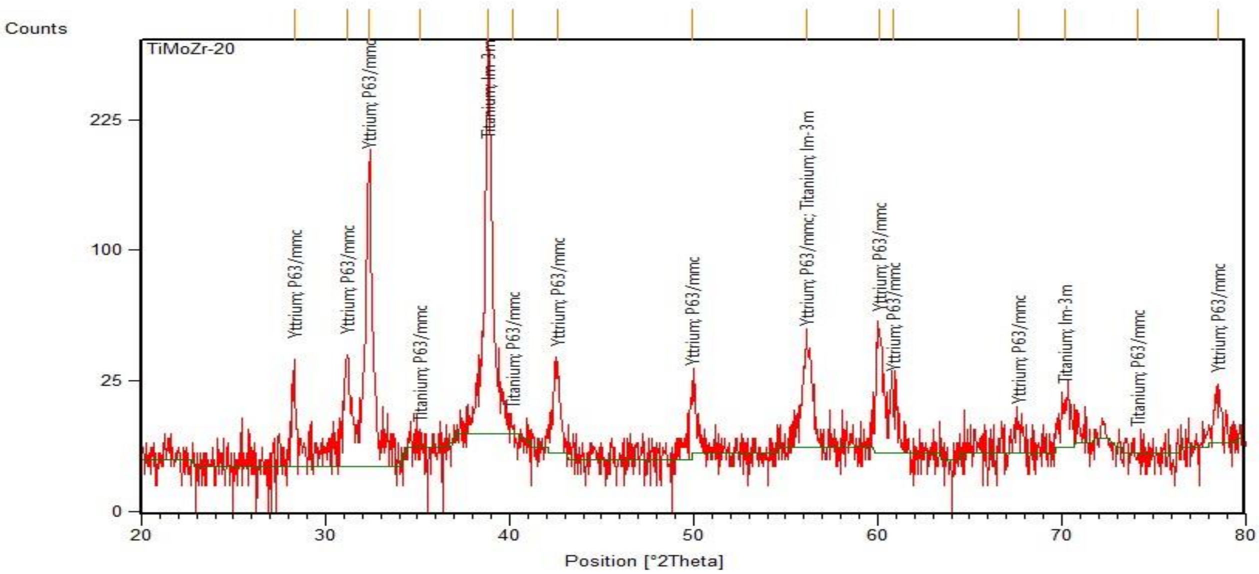

Figure 40 - Before dealloying XRD : TiMoZr 20

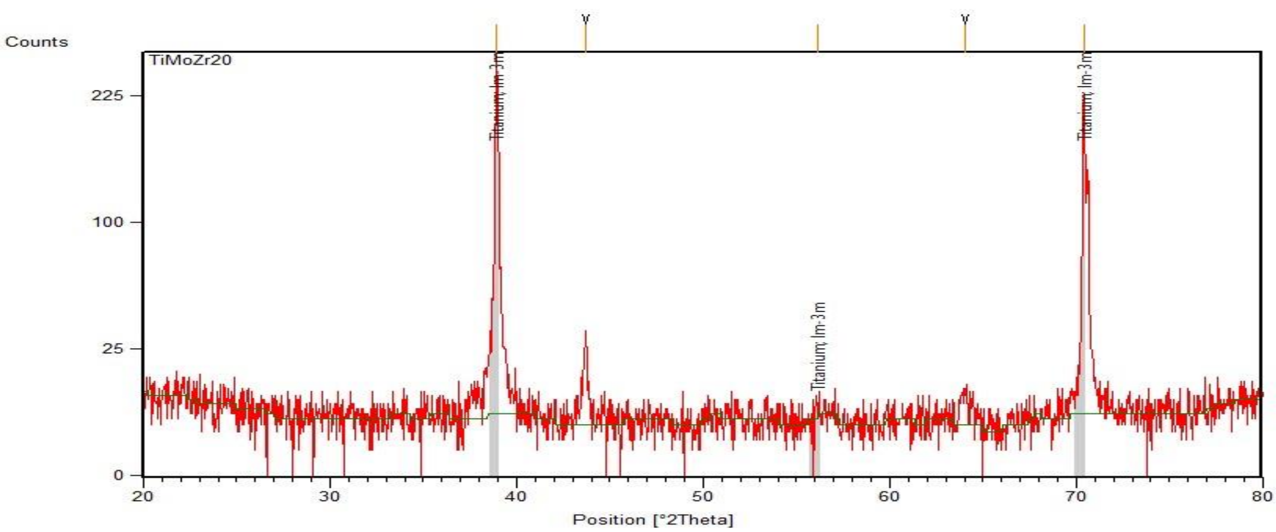

Figure 39 - After dealloying XRD : TiMoZr 20

TiMoZr-25

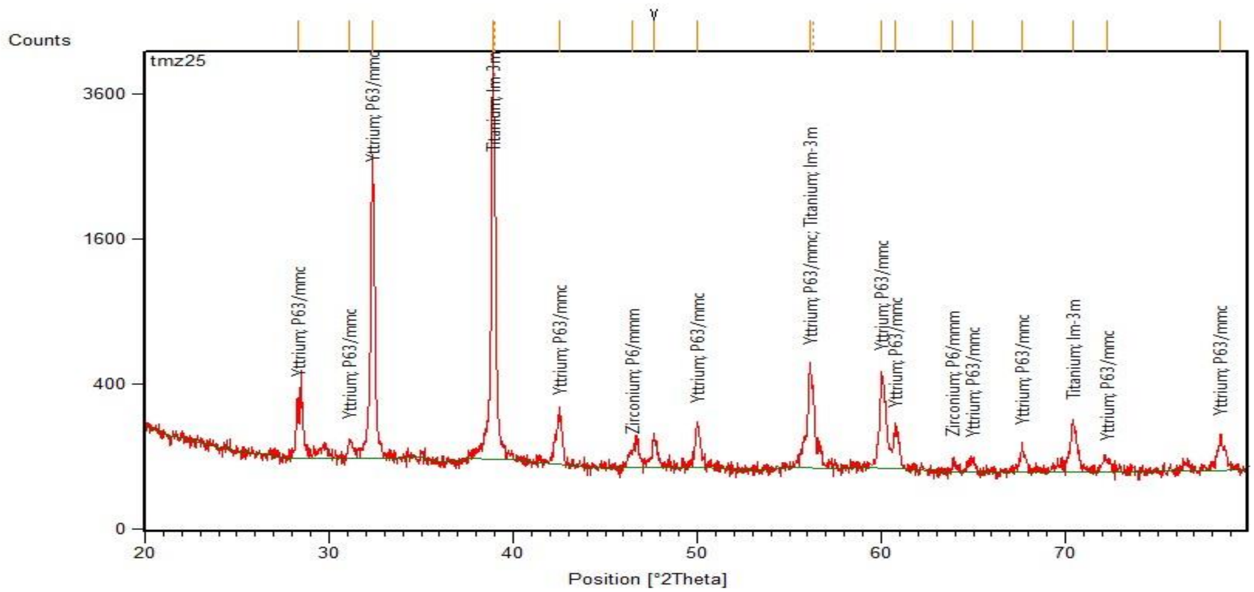

Figure 41 - Before dealloying XRD : TiMoZr 25

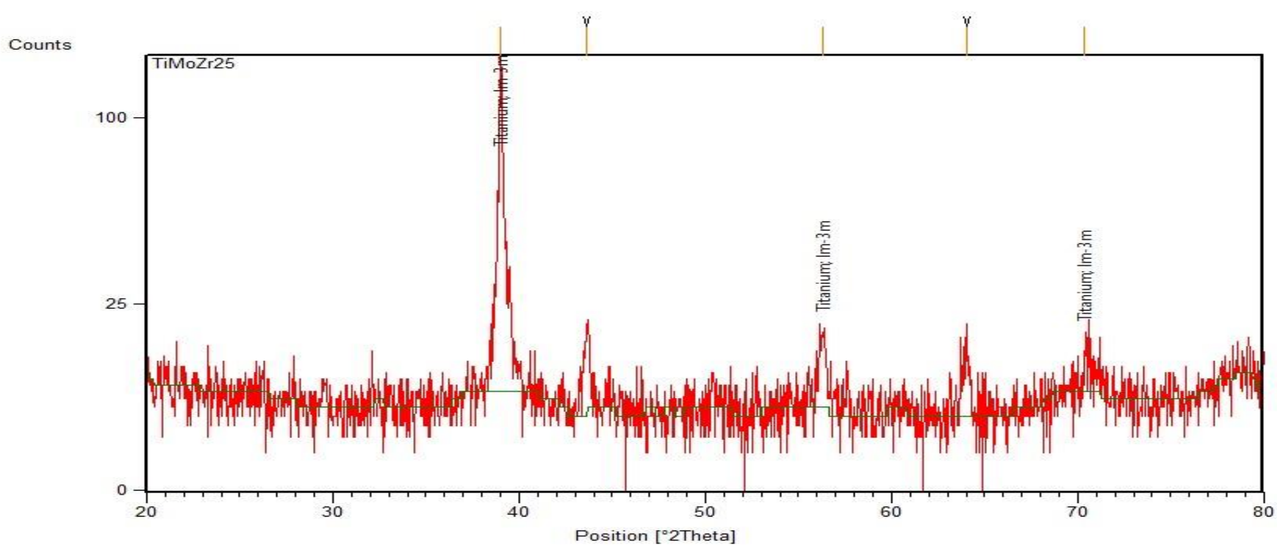

Figure 42 - After dealloying XRD : TiMoZr 25

All these results show complete removal of filler element peaks after de-alloying showing that the filler element is completely removed. There is no change in lattice parameter of alloy matrix which shows that the matrix remained unchanged. Hence, this experiment was successful in complete removal of filler and introduction of porosity.

4.3 Conclusion

Titanium-Molybdenum-Zirconium alloy was prepared with the combination of 12% Molybdenum and 6% Zirconium, successfully via arc melting. Filler material was mixed in the alloy in weight ratios from 5-25, with increments of 5. A pure TiMoZr alloy was prepared to allow us to better analyse and compare the results.

4.3.0 SEM Analysis

The SEM image revealed substantial information about the distribution of filler material within the different samples. As the amount of filler increases the valleys created by their distribution, increase as well. The size of pores created remains relatively same, in the range of 2-4 μm. This size is well within the range for successful cell implantation and travel within the body.

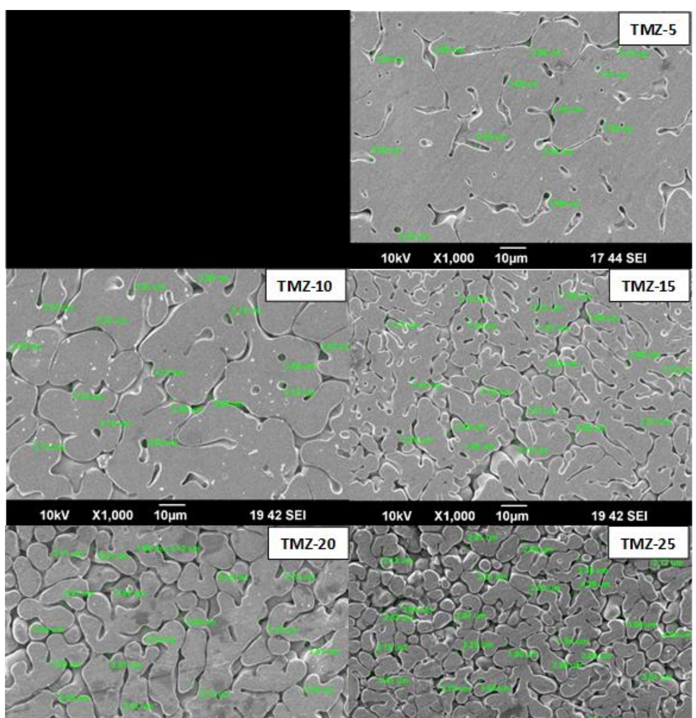

Figure 43 - SEM images with pore sizes

4.3.1 XRD Analysis

Before dealloying, the XRD peaks for all samples, except TMZ-0, showed the presence of an HCP structure. This structure corresponds to the filler material that was incorporated into the alloy samples. The evident peaks confirm that the valleys seen in the SEM image are indeed of the filler material added. The combined study of the two results yields the confirmation that the synthesis of the samples was done correctly. After dealloying, we see that all HCP peaks have been removed. This confirms that all of the filler material was removed during dealloying process. The result is a pure Ti-12Mo-6Zr biomedical porous alloy which can be used as an implant material with a higher degree of attachment.

4.4 Further Testing

4.4.0 Compression Test

In order to better understand the ability of the porous alloy to diminish the effects of stress shielding within the body. A compression test will enable us to study its mechanical properties in great detail and parameters such as young's modulus, yield strength and percent elongation can be noted. The optimum degree of porosity can then be decided.

4.4.1 Thermal Properties

Thermal diffusivity of each porous sample should be studied to find their suitability within the body. A thermal diffusivity value close to that of bone would mean low chance of dental or osteo-burn.

4.4.2 Cell Proliferation

Porous alloy samples can be placed in stimulated body fluid and subsequent cell attachment and proliferation can be studied to see effect of porosity.

4.4.3 Bio activity Test

Various tests can be performed for the titanium foams for investigating the bio activity and bio toxicity.

4.4.4 Increased porosity

Mechanical properties for increased porosity can be investigated and its impact on the biocompatibility and life of the implant.

4.4.5 Configuration of Pores

Size, shape and distribution of pores can be studied and its dependency on the physical properties of the filler metal could be investigated.

4.4.6 Surface Modification

Number of cells attached are directly linked with the contact angle and surface morphology of the specimen or structure. Various surface modifications or treatments could be another possible way to reduce the surface energy that will help in improving osteointegration for each designed sample.

4.4.7 Fatigue Study

Fatigue behavior of these foams is not yet studied which is also another important aspect in biomedical field. Human bones are involved in different types of activities due to which they face cyclic loading during the life time. This study will help to understand implant life within the body.

References

[1] **B. Henriques, Bagheri, M. Gasik, J.C.M. Souza, O. Carvalho, F.S. Silva, R.M. Nascimento. 2015.** "Mechanical properties of hot pressed CoCrMo alloy compacts for Biomedical Applications." Materials and Design.

[2] **Bish, DL and Post. 1989.** "Modern Powder Diffraction." Reviews in Mineralogy.

[3] **Hariprasad Ananth, 1 Vinaya Kundapur, H. S. Mohammed, M. Anand, G. S. Amarnath, Sunil Mankar. 2015.** "A Review on Biomaterials in Dental Implantology." International Journal of Biomedical Science 113-120.

[4] **Hendra Hermawan, Dadan Ramdan and Joy R. P. Djuansjah. 2011**. "Metals for Biomedical Applications." In Biomedical Engineering - From Theory to Applications, by Reza Fazel-Rezai.

[5] **J.R., Davis. 2003**. In Handbook of Materials for Medical devices. ASM International.

[6] **Karthika Prasad, Olha Bazaka, Ming Chua, Madison Rochford, Liam Fedrick, Jordan Spoor, Richard Symes, Marcus Tieppo, Cameron Collins, Alex Cao, David Markwell, Kostya (Ken) Ostrikov,Kateryna Bazaka. 2017.** "Metallic Biomaterials: Current Challenges and Opportunities." Materials 884.

[7] **Kim Vanmeensel, Karel Lietaert, Bey Vrancken, Sasan Dadbakhsh,. n.d**. "Additively manufactured metals for Biomedical Applications."

[8] **M.I.Z. Ridzwan, Solehuddin Shuib, A.Y. Hassan, A.A. Shokri, M.N. Mohamad Ibrahim. 2007.** "Problem of Stress Shielding and Improvement to the Hip Implant Designs: A Review." Journal of Medical Sciences 460-467.

[9] **Mitsuo Niinomi, Carl J. Boehlert. 2015**. "Titanium Alloys for Biomedical Applications." Advances in Metallic Biomaterials pp 179-213.

[10] **Mohamed Abdel-Hady Gepreel, MitsuoNiinomi. 2012.** "Biocompatibility of Ti-alloys for long-term implantation." Journal of Mechanical Behavior of Biomedical Materials.

[11] **Monika Saini, Yashpal Singh, Pooja Arora, Vipin Arora, Krati Jain. 2015.** "Implant biomaterials: A comprehensive review." World Journal of Clinical Cases 52-57.

[12] **Papavinasam, Sankara. 2014.** In Sankara Papavinasam.

[13] **Si-Young Sung, Young-Jig Kim. 2007**. "Melting and Casting of Titanium Alloys." Materials Science Forum Vols. 539-543 pp 3601-3606.

[14] **Wooley, P H, and E M Schwarz. 2004**. "Aseptic loosening." Gene Therapy 402-407.

[15] **Xiaoli Zhao, Mitsuo Niinomi, Masaaki Nakai, Takuya Ishimoto, Takayoshi Nakano. 2011.** "Development of high Zr-containing Ti-based alloys with low Young's modulus for use." Materials Science and Engineering C.

[16] **Y.J. Chen, B. Feng, Y.P. Zhu, J. Weng, J.X. Wang, X. Lu. 2009.** "Fabrication of porous titanium implants with biomechanical compatibility." Materials Letters.

[17] **Kennedy, A., 2012,** Porous metals and metal foams made from powders, in Powder Metallurgy, InTech.

[18] **Dabrowski, J.**, **2001,** Use of powder metallurgy for development of implants of Co-Cr-Mo alloy powder. Biomedizinische Technik. Biomedical engineering, **46**(4): p. 106-108.

[19] **Asaoka, K., et al., 1985,** Mechanical properties and biomechanical compatibility of porous titanium for dental implants. Journal of Biomedical Materials Research Part A, **19**(6): p. 699-713.

[20] **Banhart, J., 2001,** Manufacture, characterisation and application of cellular metals and metal foams. Progress in materials Science, **46**(6): p. 559-632.

[21] **L Reimer, 2000,** Scanning Electron Microscopy: Physics of Image Formation and Microanalysis, Second Edition, Measurement Science and Technology, Volume 11.

[22] **A. Authier, 2010,** Dynamical theory of X-ray diffraction, International Tables for Crystallography, pp. 626-646